OPEN
ASAIO Journal 2021

Real-Time Ventricular Volume Measured Using the Intracardiac Electromyogram

Marianne Schmid Daners,* Sophie Hall,* Simon Sündermann,†‡§ Nikola Cesarovic,§¶‖ Mareike Kron,¶ Volkmar Falk,†‡§‖ Christoph Starck,†# Mirko Meboldt,* and Seraina A. Dual*,**††

Left ventricular end-diastolic volume (EDV) is an important parameter for monitoring patients with left ventricular assist devices (LVADs) and might be useful for automatic LVAD work adaptation. However, continuous information on the EDV is unavailable to date. The depolarization amplitude (DA) of the noncontact intracardiac electromyogram (iEMG) is physically related to the EDV. Here, we show how a left ventricular (LV) volume sensor based on the iEMG might provide beat-wise EDV estimates. The study was performed in six pigs while undergoing a series of controlled changes in hemodynamic states. The LV volume sensor consisted of four conventional pacemaker electrodes measuring the far-field iEMG inside the LV blood pool, using a novel unipolar amplifier. Simultaneously, noninvasive measurements of EDV and hematocrit were recorded. The proposed EDV predictor was tested for statistical significance using a mixed-effect model and associated confidence intervals. A statistically significant (p = 3e–07) negative correlation was confirmed between the DA of the iEMG and the EDV as measured by electric impedance at a slope of –0.069 (–0.089, –0.049) mV/mL. The DA was slightly decreased by increased hematocrit (p = 0.039) and moderately decreased with the opening of the thorax (p = 0.003). The DA of the iEMG proved to be a significant, independent predictor of EDV. The proposed LV volume sensor is simple to integrate into the inflow cannula of an LVAD and thus has the potential to inform the clinician about the state of LV volume in real time and to automatically control the LVAD. *ASAIO Journal* 2021; 67;1312–1321

Key Words: electrocardiogram, 3D echocardiography, ventricular volume sensor, preload, LV end-diastolic volume, heart failure, left ventricular assist device, heart pump

State-of-the-art continuous flow left ventricular assist devices (LVADs) are limited in reacting to various hemodynamic states as they largely run at a constant operating speed. At a constant pump speed, the patient may experience a reduced exercise capacity and suction, followed by adverse events such as septum shift or hemolysis.[1,2] Manual titration of pump speed can improve exercise performance,[3,4] but generally only minimal improvements are achieved.[5] Automatic adaptation of pump speed is an intriguing concept but requires monitoring volume status of the patient to ensure safe operation.[4] The end-diastolic volume (EDV) has been proven as a robust parameter *in vitro*[6] and *in vivo*[7] to monitor and optimize the pump speed of LVADs. To date, there is no sensor available to measure EDV continuously.

Because EDV is difficult to measure, researchers have sought other ways to estimate EDV. The time point of the EDV coincides with the maximum electric depolarization amplitude (DA) of the heart. In theory, the measured value of the DA should be influenced by a change in the intracavitary blood pool, as stated by Brody already in the 1950s.[8–10] Hence, the maximum of the R-wave amplitude or the QRS complex is determined not only by physiologic mechanisms, such as stress, heart rate (HR), and temperature, but also by physical factors, such as the EDV.[11] The DA is preferably measured inside the LV blood pool through a unipolar noncontact intracardiac electromyogram (iEMG).[8] A unipolar measurement is required to capture the far-field response. Such a unipolar amplifier was not available until recently.[12] We hypothesize that electrodes that are integrated in the cannula of an LVAD can measure beat-to-beat

From the *Product Development Group Zurich, ETH Zurich, Zurich, Switzerland; †DZHK (German Center for Cardiovascular Research), Partner Site Berlin, Berlin, Germany; ‡Charité—Universitätsmedizin Berlin, Corporate Member of Freie Universität Berlin, Humboldt-Universität zu Berlin, and Berlin Institute of Health, Department of Cardiovascular Surgery, Berlin, Germany; §German Heart Center Berlin, Department of Cardiothoracic and Vascular Surgery, Berlin, Germany; ¶Division for Surgical Research, University Hospital Zurich and University of Zurich, Zurich, Switzerland; ‖Department of Health Sciences and Technology, ETH Zurich, Zurich, Switzerland; #Steinbeis University Berlin, Institute (STI) of Cardiovascular Perfusion, Berlin, Germany; **Radiology, Stanford University, Stanford, California; and ††Cardiovascular Institute, Stanford University, Stanford, California.

Submitted for consideration September 2020; accepted for publication in revised form March 2021.

Disclosure: Prof. Dr. Volkmar Falk has relevant (institutional) financial activities outside the summited work with following commercial entities: Medtronic GmbH, Biotronik SE & Co., Abbott GmbH & Co. KG, Boston Scientific, Edwards Lifesciences, Berlin Heart, Novartis Pharma GmbH, JOTEC GmbH, and Zurich Heart in relation to educational grants (including travel support), fees for lectures and speeches, fees for professional consultation and research, and study funds. Outside the summited work, Prof. Dr. C. Starck has received consulting fees and travel expenses from Medtronic; consulting fees and research support from Biotronik; research support from Abbott; workshop fees, consulting fees, educational grants, and research support from Cook Medical; consulting fees from Spectranetics/Philipps; and consulting fees from Angiodynamics. Dr. Seraina A. Dual, Prof. Mirko Meboldt, and Dr. Schmid Daners reports have a patent EP19169059.3 pending. The other authors report no conflicts of interest.

This study was supported by the IMG Foundation, the Bertha Schwyzer-Winiker Foundation and ETH Foundation.

Supplemental digital content is available for this article. Direct URL citations appear in the printed text, and links to the digital files are provided in the HTML and PDF versions of this article on the journal's Web site (www.asaiojournal.com).

Correspondence: Seraina Anne Dual, Tannenstrasse 3, 8092 Zürich, Switzerland. Email: seraina.dual@alumni.ethz.ch; Twitter: @dual_sera.

DOI: 10.1097/MAT.0000000000001444

EDV and thus provide additional means to monitor LV function continuously during LVAD support.[13]

In this study, we developed an LV volume sensor prototype encompassing four electrodes, which were integrated into a placeholder LVAD cannula and connected to a custom-built unipolar amplifier. Each electrode independently measured the far-field iEMG inside the LV cavity during experimentally induced, controlled hemodynamic interventions in six pigs. We report the correlation of the iEMG DA and gold-standard noninvasive measures of EDV such as echocardiography and electric impedance. Additionally, we assessed the effect of different hematocrit (HCT) levels and the effect of an open chest as potential confounders to the measurement.

Materials and Methods

Left Ventricular Volume Sensor

Four off-the-shelf pacemaker electrodes (Biotronik 25539254 IS-1 BI, Germany) were integrated into a placeholder cannula to measure the intracardiac DA in real time with no flow through it. The design of the cannula was optimized to fit with the HVAD (Medtronic, Minneapolis, MN) suture ring to facilitate surgical implantation (see **Figure 1**). The three-dimensional (3D) printed cannula was manufactured from polyamid 12 (PA12) in a selective laser sintering (SLS) process to a diameter of 20.6 mm and a length of 35 mm. The electrodes were integrated into the cannula, with two of the electrodes, B3 and B4, being shielded from the myocardium by a casket of 0.8 mm thickness. The insertion points of the electrodes were sealed with silicone (DowCorning 732).

The design of the unipolar amplifier was adapted from the recently published design of Gargiulo *et al.*[14] and tested successfully against the gold standard.[15,16] A pseudo-infinite potential is generated from a low-pass filtered signal of the reference electrodes, which can be arbitrarily chosen among the electrodes B1–B4. All four signals are then referenced to this pseudo-infinite potential, rendering a pseudo-unipolar electromyogram. A schematic of the electronic circuit is shown in **Figure 2**. The main advantage of using this unipolar amplifier is that the unipolar measurement is obtained from two implanted electrodes, rather than referenced to a data acquisition unit.[16] In this study, the reference electrode was chosen per animal as the one which proved the most stable at the beginning of each trial.

Experimental Setting

The cannula prototype was tested in acute pig models (n = 6, female, Swiss large white; see **Table 1**). The animal housing and all procedures and protocols were approved by the Cantonal Veterinary Office (Zurich, Switzerland) under the license number 219/2016. Animal housing and all experimental procedures were in accordance with Swiss animal welfare protection law, and conform to European Directive 2010/63/EU of the European Parliament and the Council on the Protection of Animals used for Scientific Purposes, and to the Guide for the Care and Use of Laboratory Animals.

After loss of postural reflexes following premedication with ketamine (15 mg/kg), midazolam (0.5 mg/kg), and atropine (0.1–0.2 mg/kg) anesthesia was deepened by an intravenous bolus injection of propofol (1–2 mg/kg body weight) and the animals were intubated. General anesthesia was maintained with propofol (2–5 mg/kg/h, i.v.) in combination with isoflurane (1–2.5%) by positive pressure ventilation in an air–oxygen mixture (1:1, 4–6 L/min) with an inspired oxygen fraction (FiO_2) of 0.5, tidal volume of 6–8 ml/kg, a frequency of 10–15 bpm and a positive end-expiratory pressure (PEEP) of 5 cmH_2O. For intraoperative analgesia, buprenorphine (0.01 mg/kg body weight) was administered intravenously approximately 30 minutes before the first skin incision and was continued throughout anesthesia. During surgery, animals received a continuous intravenous infusion of crystalloids (5–7 ml/kg/h).

For maximum control of hemodynamics, a modified cardiopulmonary bypass (CPB) was installed without oxygenator. A shunt connected the outlet and inlet line of the CPB, which could be clamped according to whether it was intended to decrease or increase volume load. Drainage and inlet were preformed *via* a single femoral vein access realized by inserting a venous CPB-cannula in the animal's femoral vein. The circuit was used to rapidly load or unload the animal's circulation. After lower hemi-sternotomy was performed for access, the cannula prototype was implanted into the LV at the apex,

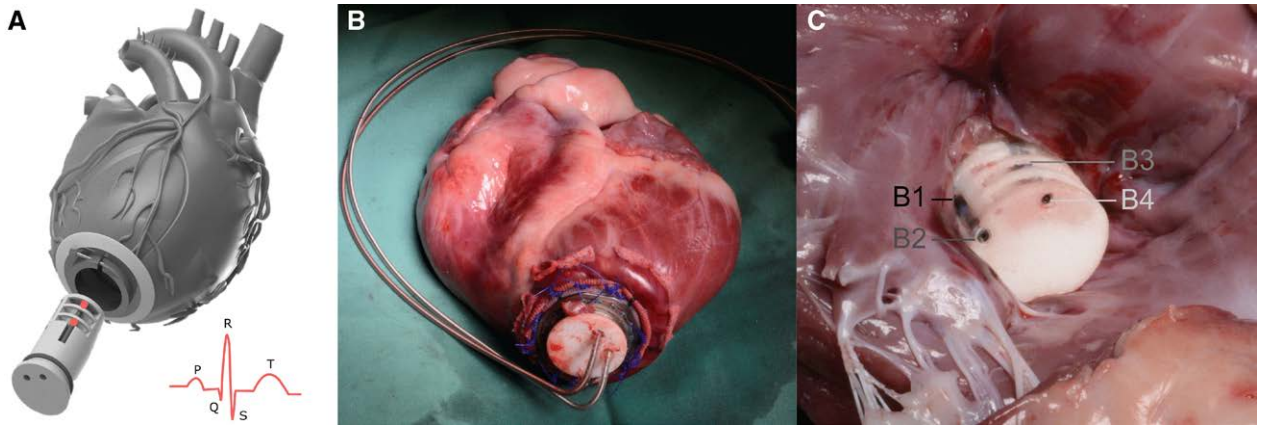

Figure 1. Surgical implantation. **A:** A cannula encompassing four electrodes (B1–B4) was implanted in the left ventricular cavity. The electrodes measured the intracardiac electromyogram (iEMG). **B:** Explanted heart showing the attachment with an HVAD suture ring. (C) Intracavity view of the cannula showing the shielded (B3, B4) and unshielded electrodes (B1–B2).

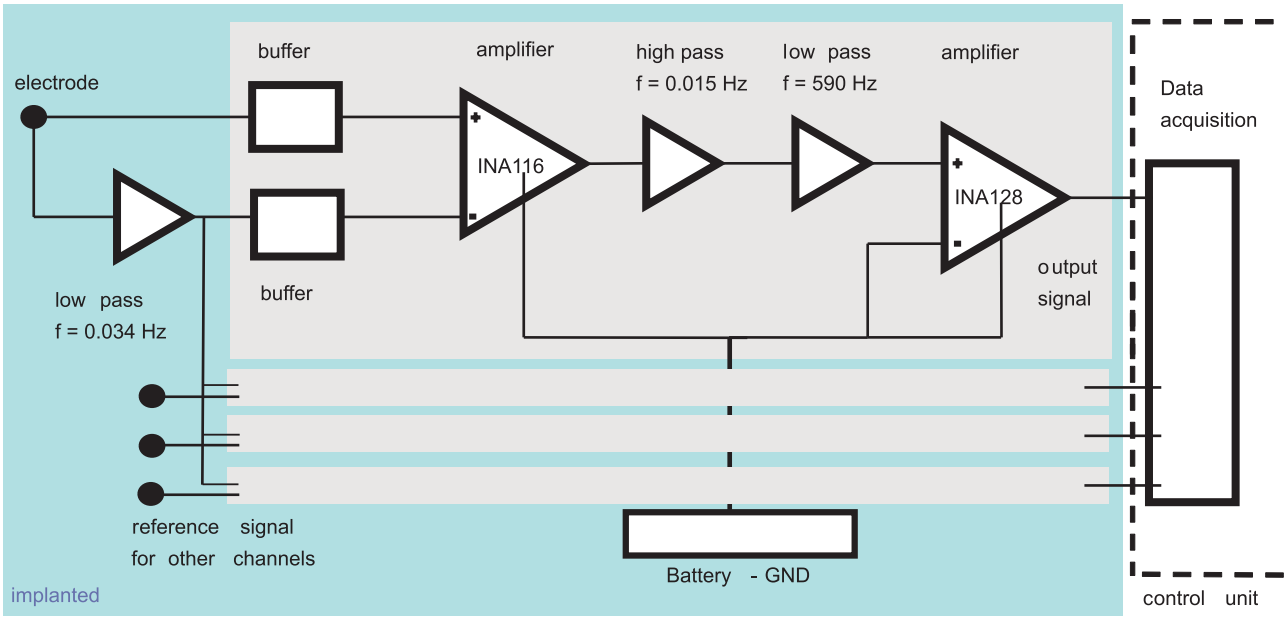

Figure 2. Design of the unipolar amplifier. The reference electrode is referenced to its own low-pass filtered signal. The low-pass filtered signal is further used for the other three electrodes. The amplifier consists of two amplifier stages and two filters.[15,16]

using an HVAD suture ring (Medtronic), and thus mimicking an LVAD implant. After completion of both surgical steps, the thoracic spreader was removed, and the suprasternal tissue closed using sutures, whereas the pericardium and the sternum were left open. The thorax was reopened only if necessary, to stabilize or resuscitate the animal. A balloon catheter (Medtronic, Reliant 12 Fr Balloon) was inserted in the descending aorta to allow for temporary partial or full aortic occlusion to control for afterload. After the acute trial the animal was euthanized with penthobarbiturat 75 mg/kg Esconarkon (Streuli Pharma AG, Uznach, Switzerland).

Four types of experimentally induced hemodynamic interventions were performed to simulate changes in pre- and afterload and hence, changes in EDV: *Small* ΔV, *Large* ΔV, *Occlusion* of the descending aorta using a balloon catheter, and *Hemorrhage* (see **Figure 3**). The sequence of interventions performed per animal was randomly assigned (see **Table 1**). The amount of blood in the circulation was altered by draining or infusing blood into the venous system using the CPB followed by a 5 minutes stabilization period to allow for steady-state conditions. The *small* ΔV consisted of steps of 200 ml; the *large* ΔV were randomized with a maximum step of 1,500 ml. The interventions with *small* ΔV were designed to keep HCT values in a range of ±2.5% from baseline. Dynamic measurements were recorded during the *occlusion* intervention. In three animals, we aggressively reduced the HCT by inducing a *hemorrhage* and subsequent infusion of NaCl 0.9% at the last intervention.

Data Acquisition and Analysis

At each intervention a breath-hold was initiated and the measured DA from the intracardiac electrodes was compared with the EDV measured through electric impedance (EDV_{imp}) and transesophageal echocardiography (EDV_{echo}). All continuous electrophysiologic data were recorded with the SIGMA A-M signal conditioner at 2 kHz and acquisition was triggered manually at each intervention for synchronization

Table 1. Experiments Conducted

	No.	Intervention	Thorax	n	HCT (mV/%)	HR (bpm)	CVP_{sys} (mmHg)	Fem_{sys} (mmHg)
Animal 1	I	Small ΔV	closed	6	24.5 ± 1.0	90.8 ± 4.3	13 ± 1	45 ± 15
Animal 2	I	Small ΔV	open	14	29.1 ± 2.6	93.2 ± 9.1	16 ± 3	51 ± 8
	II	Hemorrhage	open	5	19.8 ± 3.9	83.9 ± 23.0	14 ± 1	49 ± 11
Animal 3	I	Small ΔV	closed	18	24.6 ± 1.6	46.8 ± 2.8	19 ± 2	75 ± 7
	II	Occlusion	closed	10	23.8 ± 1.0	79.8 ± 10.0	n/a	n/a
	III	Large ΔV	closed	6	23.0 ± 1.5	98.0 ± 3.3	19 ± 2	60 ± 14
	IV	Hemorrhage	closed	6	20.2 ± 4.1	87.8 ± 16.0	20 ± 2	45 ± 13
Animal 4	I	Small ΔV	closed	16	25.4 ± 1.6	56.2 ± 9.6	18 ± 3	64 ± 19
	II	Occlusion	open	7	24.1 ± 0.4	52.7 ± 1.2	18 ± 2	41 ± 16
	III	Large ΔV	open	2	22.0 ± 0.0	50.4 ± 2.7	17 ± 3	41 ± 23
Animal 5	I	Small ΔV	closed	17	27.5 ± 1.5	74.3 ± 12.0	n/a	70 ± 11
	II	Occlusion	closed	8	24.0 ± 0.0	90.5 ± 3.8	n/a	70 ± 15
Animal 6	I	Small ΔV	closed	10	25.1 ± 1.3	56.7 ± 5.3	16 ± 3	69 ± 13
	II	Large ΔV	closed	9	22.6 ± 1.7	70.3 ± 8.9	16 ± 6	42 ± 22
	III	Hemorrhage	closed	9	17.4 ± 5.4	67.5 ± 22.0	19 ± 4	46 ± 21

n, number of interventions performed; HCT, hematocrit; HR, heart rate; CVP, central venous pressure; Fem, femoral pressure; sys, systolic; mean +/- standard deviation

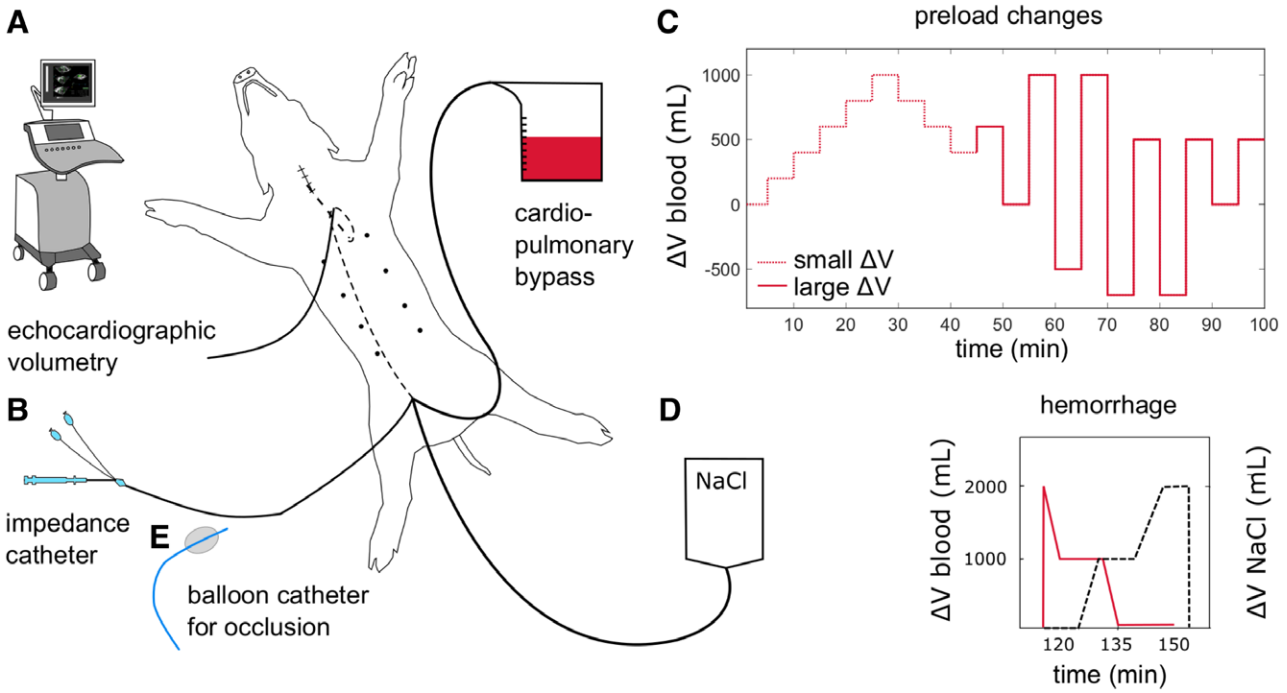

Figure 3. Experimental protocol. During all interventions, left ventricular volume was recorded through (**A**) echocardiography and (**B**) electric impedance. (**C**) The amount of blood in the circulation was altered using a cardiopulmonary bypass resulting in small and large changes in volume (ΔV). (**D**) The hematocrit was altered using hemorrhage and subsequent reinfusion of 0.9% NaCl. (**E**) Afterload was increased using a balloon catheter.

purposes. Potentials from the intracardiac electrodes were recorded alongside with continuous measurements of all three main leads of the surface electrocardiogram (ECG). LV pressure and LV impedance were measured by a pig-tail catheter (CL-71083-PL; BP Hengelo, The Netherlands) (see **Figure 3B**) and were recorded *via* a Windows machine running the Leycom conduct NTV3.18 data logger (Leycom; BP Hengelo) at 250 Hz. The echocardiographic transesophageal probe (Philips CX50; Philips, The Netherlands) was positioned inside the pericardium posterior to the heart and served for two-dimensional (2D) echocardiographic measurements of LV EDV and LV end-systolic volume (ESV). The HCT was measured at each intervention using a Statspin Multipurpose centrifuge (Stat Spin MP, Provet, Switzerland). The blood sample was centrifuged at 15,800 rpm for 120 seconds and the packed cell volume was determined using a micro HCT tube reader.

All data were postprocessed and filtered in MATLAB (R2019a; The Mathworks Inc., Natick, MA). The resulting signal quality is shown in two exemplary waveforms in **Figure 4** accounting for high and low preload conditions. The QRS complex was detected in Lead I of the surface ECG and used to cut all continuous signals into heartbeats. Per beat, we identified EDV and ESV in the electric impedance signal as maximum and minimum. The DA in the signals acquired by each intracardiac electrode was found by relating it to the isoelectric level. The isoelectric level was taken as the median value of a 315 ms long segment occurring after the P-wave and before the depolarization. The DA was found in a specified time interval as the negative peak, defined by a threshold and the peak prominence. Per intervention, we report the median of the beat-wise data over a period of 15 seconds.

Statistical Methods

All summary statistics in **Table 1** are reported as mean ± standard deviation.

A mixed-effect model was used to describe the relationship between DA and the EDV in MATLAB (see **Equation 1**). The linear relationship is described by two parameters: an offset, or *y*-axis intercept, (μ), and the slope (β). A mixed-effect model assumes a fixed underlying relationship (μ, β), while it allows for subject-specific variation in parameters (μ_i, β_i), also known as random intercept–random slope model:

$$DA_{ij} \sim (\mu+\mu_i)+(\beta+\beta_i)\ EDV_{ij} \quad (1)$$

The residual variance and all estimated parameters are reported with 95% confidence intervals (CIs).

The model was fit using *small ΔV* and *large ΔV* at the same time. One separate model was fit for EDV based on echocardiography and electric impedance. The most stable intracardiac electrode was chosen per animal for analysis of the DA and reported in the analysis. The electrodes were electrode B4 for animals 1, 2, 5, 6; electrode B3 for animal 2; and electrode B3 for animal 3. The estimated subject-specific parameters were subsequently validated in real time for the *occlusion* interventions, if available.

An extended mixed-effect model estimated the effect of potential confounders (open chest, change of HCT, and HR).

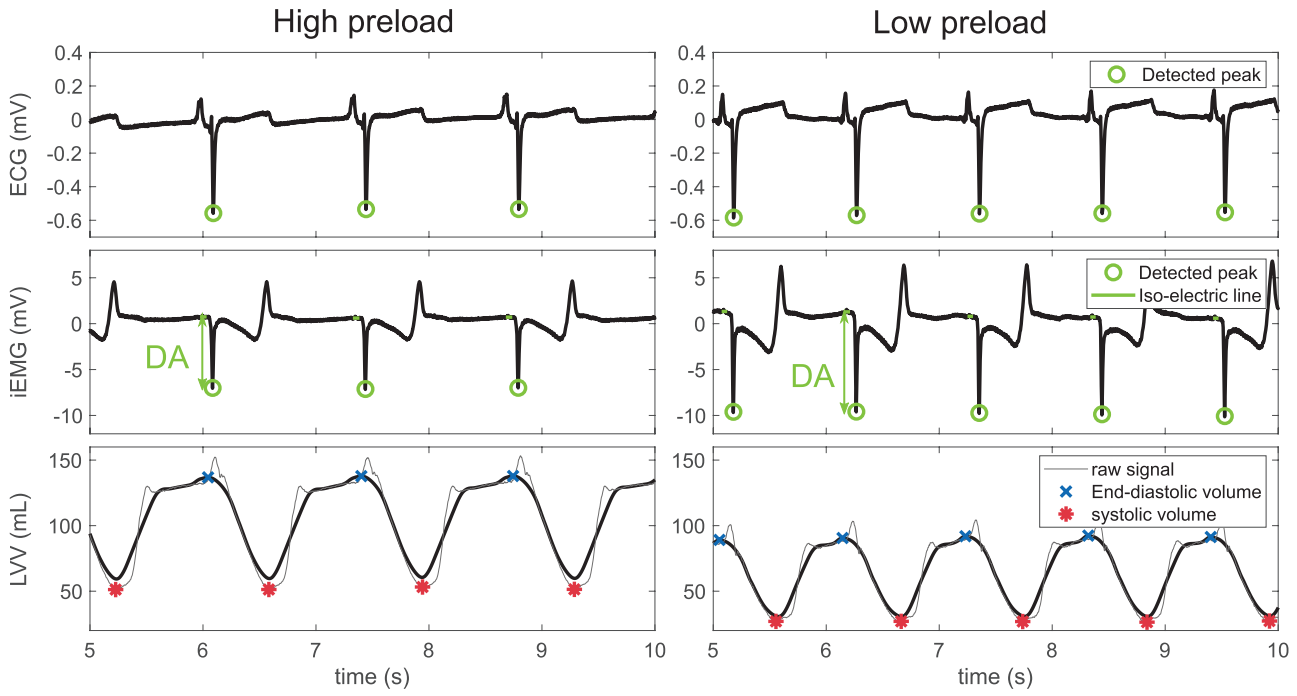

Figure 4. Recorded waveforms. Representative waveforms are obtained from the electrocardiogram (ECG), the intracardiac electromyogram (iEMG), and the left ventricular volume (LVV) using electric impedance. Data are obtained from animal 3 at a high (left) and low (right) preload state. DA, depolarization amplitude.

For this analysis, data from *small ΔV* and *large ΔV* as well as *hemorrhage* were used.

Results

DA and EDV

Per animal, the observed range of DA was up to 6 mV, whereas the EDV range was up to 80 ml during *small ΔV* and *large ΔV*. Using the novel LV volume sensor, the EDV was found to be a significant predictor of the DA. This was true for the EDV measurement for both the electric impedance (p = 3e–07) and echocardiographic volume measurement (p = 1e–04) and showed excellent agreement (R^2 = 0.85 and R^2 = 0.83, respectively) (see **Table 2**). The mean estimation error was found to be 14.6 and 15.9 ml, respectively, with CIs of 29.2 and 31.8 ml. Animal 2 showed an increased mean-square error, compared with the other animals (26.9 ml *vs.* [15.2, 5.0, 12.7, 2.3, 4.1 ml]; see Figure S1, Supplemental Digital Content 1, http://links.lww.com/ASAIO/A630). In animal 2, the surface ECG showed high waveform variability and electric impedance volume measurement was unreliable compared with echocardiography. Also, the iEMG recordings showed high variability of DA across one 15 second segment and the waveforms between electrodes and beats were distinctly different. Excluding animal 2, the mean-square error reduces to 7.9 and 7.6 ml, for EDV_{imp} and EDV_{echo}, respectively, resulting in CIs of 15.8 and 15.2 ml, respectively.

The estimated slopes and intercepts of the fixed model are comparable between echocardiography and electric impedance (see **Table 2**). The estimated offset (μ) shows high variability in the animal-specific models (colored line) compared with the fixed model (black line), as can be observed in **Figure 5**. For electric impedance, the estimated slope shows low variability between animals, observable by the parallel slopes of the fixed and animal-specific models in **Figure 5**. In contrast, the variability in animal-specific slopes is higher for volume estimated by echocardiography (see Figure S2, Supplemental Digital Content 1, http://links.lww.com/ASAIO/A630). The results per animal can be found in Table S1 (Supplemental Digital Content 1, http://links.lww.com/ASAIO/A630).

Position of the Electrode

All electrodes recorded the iEMG electrogram well, independent of their position on the cannula. Example waveforms can be found in **Figure 6**. We found up to 75% of the continuous signals to be permissible (see **Figure 6A**). In 6% of cases, the heart rhythm of the animal was unstable, in 17% we observed large jumps in the DA amplitude and the remaining signals were excluded due to technical issues. Electrodes B1 and B2 were not shielded from interaction with the myocardium. The measured DAs were highly correlated between the electrodes across the four positions B1–B4 (see **Figure 6B**). The electrode position affected the offset of the DA, but not its relationship with the EDV (see **Figure 6C**).

Impact of Open Chest, HCT, and the HR

The impact of different HCT levels and open chest are reported in **Table 1**. The HCT was recorded during each intervention, in order to assess its influence on the DA. The levels of HCT remained stable during the *small ΔV*. During the *large ΔV* and especially during *hemorrhage,* higher changes in HCT were expected and recorded. In animals 2, 3, and 6, the HCT was reduced to 16%, 16%, and 10%, respectively, at the end

Table 2. Mixed-Effect Model Parameters

	Estimate	CI–	CI+	SE	*p* value
EDV_{imp}					
Intercept, μ (mV)	15.5	13.0	17.9	1.45	2e–17
EDV, β (mV/mL)	–0.069	–0.089	–0.049	0.013	3e–07
Animal residual SD	0.99	0.84	1.17	–	–
EDV_{echo}					
Intercept, μ (mV)	14.4	11.9	16.9	1.41	9e–17
EDV, β (mV/mL)	–0.072	–0.104	–0.040	0.018	1e–04
Animal residual SD	1.05	0.90	1.23	–	–

CI, confidence interval; EDV_{imp}, end-diastolic volume measured by electric impedance; EDV_{echo}, end-diastolic volume measured by echocardiography; SD, standard deviation; SE, standard error.

of the experiment. Using data from the *small ΔV* and *large ΔV* as well as *hemorrhage* in these three animals, the HCT was found to be a significant predictor ($p = 0.039$) of the DA with an estimated effect of 0.06 mV/% (see **Table 3**). However, if only data from the *hemorrhage* intervention were considered, both EDV and HCT did not show significant correlation with the DA. The intracardiac DA was further confounded by the chest being open or closed. Opening of the chest was found to decrease the measured DA by 2.1 mV in the extended mixed-effect model. The HR did not significantly affect the DA.

Dynamic Response to Occlusion Maneuver

The animal-specific models obtained from the observations during the *small ΔV* and *large ΔV* interventions (**Table 2**) were used to estimate volumes (EDV_{iEMG}) based on the DA during an *occlusion* maneuver performed in three out of the six animals. **Figure 7** shows the dynamic response to the *occlusion* maneuver for the three animals 3, 4, and 5, for animal 4 the thorax was open. The estimated volumes from the intracardiac EDV_iEMG can detect changes in EDV_{imp} well during acute occlusion of the descending aorta (see **Figure 7**). No time delay is observed between the intervention-based increase in EDV and the decrease in the DA of the iEMG signal.

Discussion

The intracardiac DA was found to be a strong predictor of beat-wise EDV, when measured by the proposed LV volume sensor. The CIs of estimating EDV using the LV volume sensor were found to be 16 mL. Hence, the accuracy is comparable with the intraobserver variability reported for clinical 2D/3D echocardiography (18/12 mL).[17,18] The effect was observable in all four electrodes, with variable sensitivity.

Large variation in subject-specific parameters implies that subject-specific calibration is necessary. Every subject requires independent calibration of the LV volume sensor, due to blood composition, electrode placement, and heart size. The EDV measured by the LV volume sensor can discern sudden changes in hemodynamics, for example, filling of the heart

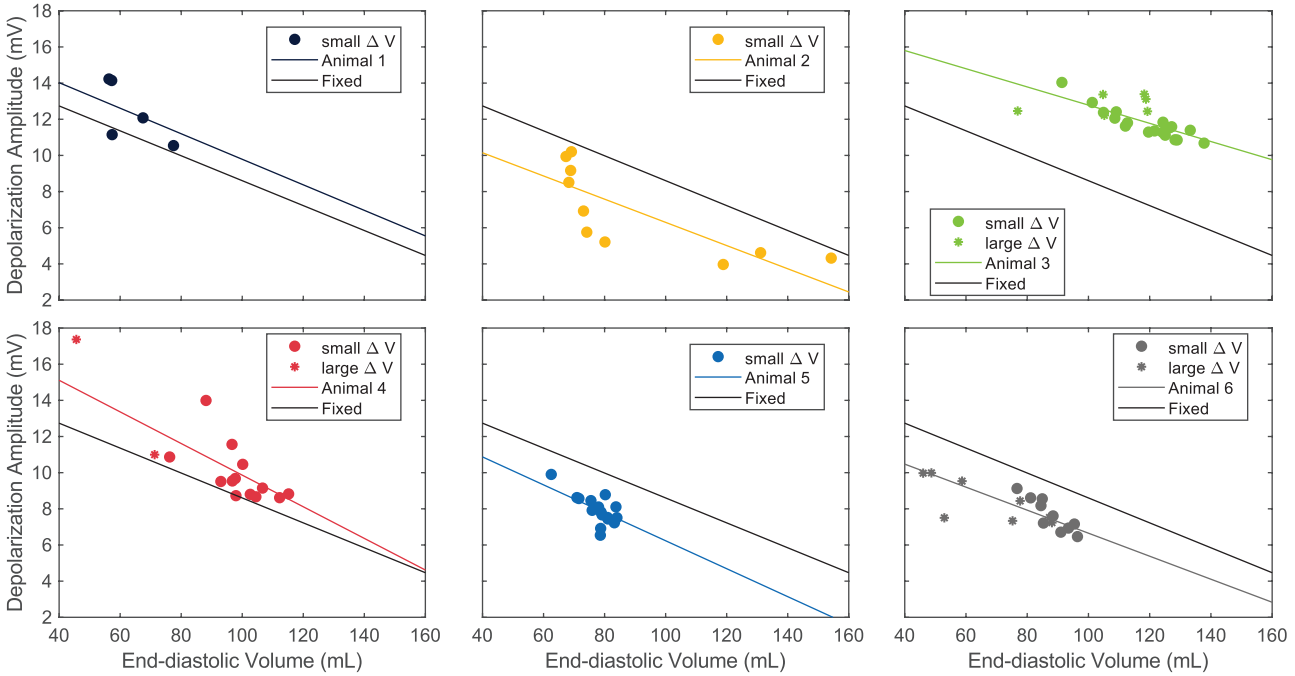

Figure 5. The depolarization amplitude and the end-diastolic volume (EDV). A mixed-effect model relates the depolarization amplitude of the intracardiac electromyogram with the end-diastolic volume measured by electric impedance. Each measurement point represents the median of a steady-state segment of 15 seconds.

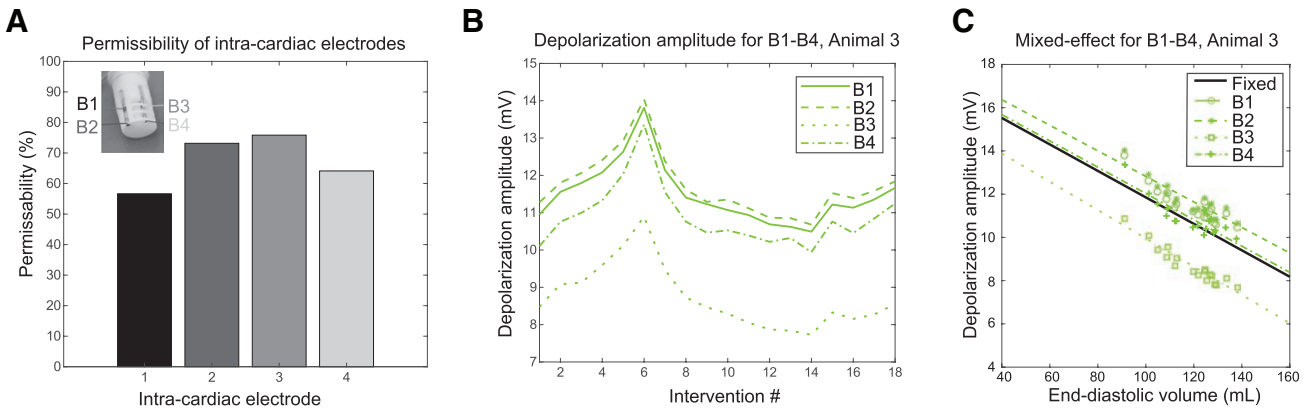

Figure 6. Positioning of the electrodes. **A:** The number of permissible intracardiac electromyogram recordings varied across the different electrodes B1–B4. Electrodes B3 and B4 were shielded from the blood pool, by a three-dimensional (3D) printed cage. **B:** The depolarization amplitude (DA) varied consistently over time. **C:** The offset of the relationship between the DA and the end-diastolic volume is preserved, whereas the offset differs across electrodes. Includes data only from small ΔV.

upon occlusion of the descending aorta. The study was further able to quantify the effect of the HCT as well as chest configuration on the LV volume sensor measurement. Integration of the LV volume sensor into implantable devices, such as an LVAD, might inform patients and clinicians on beat-to-beat hemodynamics.

Electrodes can be integrated into medical devices without additional surgical trauma. Full integration of sensors into an LVAD is key to prevent any additional surgical maneuver that could either put the patient at additional risk or delay the conduct of surgery. This study is not the first to attempt to integrate a sensor within an LVAD. Various groups have attempted the integration of pressure sensors into the cannula, but the interface of the sensor with the blood has not been easily achieved.[19,20] Additionally, experience of the community remains limited with drift in readings from implantable pressure sensors over long periods of time. Some well-established pressure sensors such as CardioMEMS allow only for discontinuous data recording, making them unsuitable for LAVD control.[21] In contrast, the proposed LV volume sensor relies on established implantable sensor technology, that is, pacemaker electrodes. This study provides evidence, that due to their small size and off-the-shelf availability, pacemaker electrodes can be integrated into the cannula of an LVAD.

Alternative, integrated measurement technologies for preload in LVADs are scarce. End-diastolic pressure is a valid estimate of preload. However, end-diastolic pressure is less sensitive than EDV to changes in preload measured in relative terms. Alternatively, intracardiac ultrasound is capable of directly measuring distances inside the heart, which is at once/on the one hand a highly desirable measure.[22,23] At the same time, such a sensor is technically complex and generates large amounts of data, because of the high-resolution. Haines *et al.*[24] have been able to use pacemaker leads in patients to measure bipolar impedance, and thereof estimate EDVs and ejection fractions with high accuracy. The technology requires a pacemaker to be implanted and is not yet clinical standard. Impedance has also been integrated into the cannula of an LVAD and successfully tested *in vivo*.[25] The measurement was, however, limited to measuring apical blood volumes, as the electric field for measurement is only spanned in the apex. On the contrary, the unipolar amplifier measures the far-field and thus enables the measurement to also be sensitive to changes in volume in the mid-ventricle.[10] The LV volumes sensor further takes advantage of the electric field spanned by the heart's own activity. Like with impedance, the proposed methodology requires a subject-specific calibration.

Table 3. Confounders to the Depolarization Amplitude in Animals 2, 3, and 6

	Estimate	CI–	CI+	SE	*p* value
Intercept (mL)	17.1	14.52	19.6	1.285	7.49e–22
EDV (mV/mL)	–0.0661	–0.080	–0.052	0.007	1.93e–14
HCT (mV/%)	–0.0609	–0.118	–0.002	0.029	0.039
Open chest (mV)	–2.1	–3.4	–0.7	0.687	0.003

The model was fitted with data from the small and large changes in volume as well as the hemorrhage intervention.
EDV, end-diastolic volume; HCT, hematocrit; CI, confidence interval; SE, standard error.

In clinical practice, the LV volume sensor constitutes an excellent complement to echocardiography. Echocardiography is the established method to measure left- and right-sided volumes, useful to titrate the speed of an LVAD. Theoretically, measurement of geometry using speed of ultrasound is highly accurate. But transthoracic echocardiography is sensitive to patient echogenicity, requires experience in effective probe placement, and is especially difficult in patients with an LVAD due to artifacts from shadowing. Still, it remains the only non-invasive measurement for hemodynamics at the bedside to date. Transesophageal echo shall be used for patient-specific calibration post-LVAD implantation. Transthoracic echocardiography will remain the go-to technology for recalibration after early ventricular remodeling in the first 4 weeks. During this time, the LV volume sensor needs to be frequently recalibrated using echocardiography to find the patient-specific offset and slope. Once, the patient is stable and at home, the LV volume sensor can provide continuous information on EDV even in the remote setting.

In heart failure patients, physiologic variation in QRS amplitude measured in the surface ECG were previously reported to be ±0.3 mV.[26] Based on the sensitivity of 0.07 mV/mL found in this study, the proposed technology can discern volume changes as small as 4 mL. The same study reported that

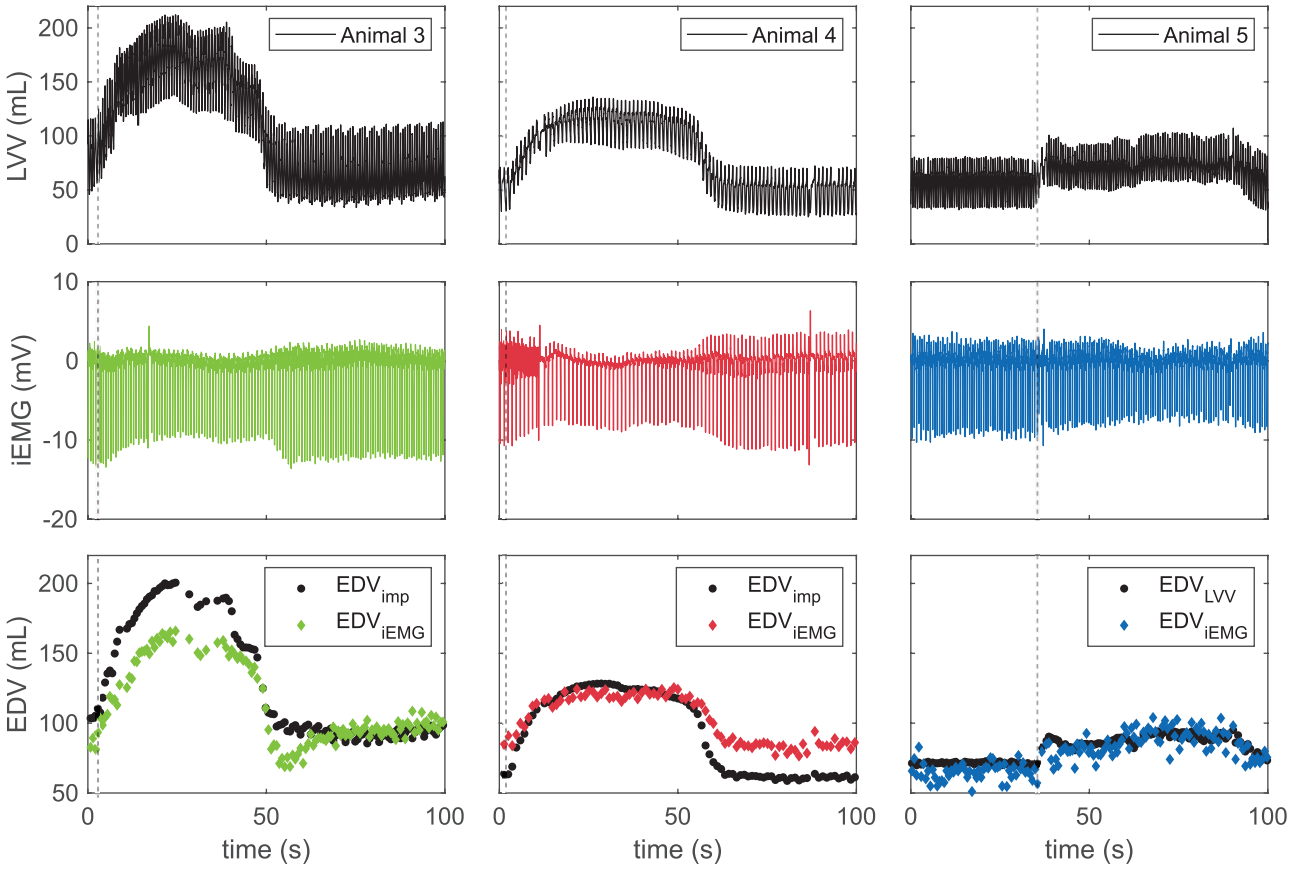

Figure 7. The intracardiac electromyogram (iEMG) during dynamic change in afterload during occlusion of the descending aorta (dashed line). One out of three representative occlusion maneuver is depicted per column for animal 3, animal 4, and animal 5. The beat-wise end-diastolic volume (EDV) was estimated using the iEMG and compared against the EDV_{imp} derived from the left ventricular volume (LVV) signal measured by electric impedance.

variability in QRS amplitude in the surface ECG remained unaffected by pacing.[26] As is evident, the LV volume sensor is likely to detect and report severe adverse events such as extreme LV emptying or overload conditions.

Electrode positioning, opening of the chest, and HCT have been shown to confound the Brody effect in previous studies and are therefore addressed extensively in this study. The reliability of electrodes shielded from the blood pool was not different from the unshielded electrodes. Potentially the shielded electrodes were less likely to be exposed to the myocardium, but blood clotting might have affected the measurement. Although the positioning of the electrode altered the overall levels of the DA, the slope was sustained. Based on the findings in this study, the exact positioning is not critical, and how electrodes shall be shielded needs further investigation.

One previous study in dogs found a relationship between the endocardial EMG measurements and EDV which was negative for the endocardium, positive for the surface ECG and showed no effect in the epicardium.[27,28] Changes in epicardial DAs were around 20%, following pharmacologically induced increases in HR and without reporting the HCT. In our study, volume changes were induced solely by infusion of blood to keep blood conductivity constant. HCT levels remained within 5%. The relative changes in DA were comparable (~30% per animal). Another study in pigs also found sensitivities of 0.03–0.09 mV/mL in an open chest configuration.[13] Our study did not include the effect of the RV blood volume nor blood flow in the LV, but this aspects should be addressed in the future.

In summary, beat-to-beat volume measurement might provide critical information in the management of patients with an LVAD. The current study provides evidence that an LV volume sensor can be easily integrated into an LVAD inflow cannula and provide information on acute changes in LV volume and is indicative for adverse events such as extreme LV emptying or overload. Using the LV volume sensor to automatically and physiologically adapt the pump speed to the patient's need is highly desirable. Given the manifold determinants of the QRS amplitude, the LV volume sensor signal should be preferably used in combination with a mechanical signal such as pump flow, LV pressure or ultrasound distances to further increase robustness. Furthermore, the effects of long-term drift need to be accounted for in the interpretation of such a signal. Future research should also investigate whether similar measurements could be obtained from pacemaker leads to measure right and left ventricular volumes. As the physical origin of the observed effect remains incompletely understood, the current study assumes a linear relationship between the DA and the EDV. More detailed modeling studies can help elucidate the underlying relationship. In the next step, this LV volume sensor will be tested in interaction with an LVAD and in a heart failure model.

Acknowledgment

The authors thank Dominic Jacob for support with the design of the pseudo-unipolar amplifier; Sara Mettler for her technical help; the Seminar for Statistics at ETH Zurich for their statistical support and advice; and the IMG Foundation, the Bertha Schwyzer-Winiker Foundation, and ETH Foundation for their financial support. This project is part of the Zurich Heart project under the umbrella of University Medicine Zurich.

References

1. Reesink K, Dekker A, Van der Nagel T, *et al*: Suction due to left ventricular assist: Implications for device control and management. *Artif Organs* 31: 542–549, 2007.
2. AlOmari AH, Savkin AV, Stevens M, *et al*: Developments in control systems for rotary left ventricular assist devices for heart failure patients: A review. *Physiol Meas* 34: R1–R27, 2013.
3. Jung MH, Hansen PB, Sander K, *et al*. Effect of increasing pump speed during exercise on peak oxygen uptake in heart failure patients supported with a continuous-flow left ventricular assist device. A double-blind randomized study. *Eur J Heart Fail* 16:403–408, 2014
4. Apostolo A, Paolillo S, Contini M, *et al*: Comprehensive effects of left ventricular assist device speed changes on alveolar gas exchange, sleep ventilatory pattern, and exercise performance. *J Heart Lung Transplant* 37: 1361–1371, 2018.
5. Fresiello L, Buys R, Timmermans P, Vandersmissen K, Jacobs S: Exercise capacity in ventricular assist device patients : Clinical relevance of pump speed and power. *Eur J Cardiothorac Surg* 50: 752–757, 2016.
6. Petrou A, Lee J, Dual S, Ochsner G, Meboldt M, Schmid Daners M: Standardized comparison of selected physiological controllers for rotary blood pumps: *In vitro* study. *Artif Organs* 42: E29–E42, 2018.
7. Ochsner G, Wilhelm MJ, Amacher R, *et al*: In vivo evaluation of physiologic control algorithms for left ventricular assist devices based on left ventricular volume or pressure. *ASAIO J* 63: 568–577, 2017
8. van Oosterom A. Macroscopic source descriptions. In: Macfarlane PW, van Oosterom A, Pahlm O, Kligfield P, Janse M, Camm J, eds. *Comprehensive Electrocardiology*, 2011th edn. London: Springer Verlag, 2010, pp. 193–225.
9. van Oosterom A, Plonsey R: The Brody effect revisited. *J Electrocardiol* 24: 339–348, 1991.
10. Brody DA: A theoretical analysis of intracavitary blood mass influence on the heart-lead relationship. *Circ Res* 4: 731–738, 1956.
11. Schijvenaars BJA, van Herpen G, Kors JA. Intraindividual variability in electrocardiograms. *J Electrocardiol* 41: 190–196, 2008.
12. Gargiulo GD, McEwan AL, Bifulco P, *et al*: Towards true unipolar ECG recording without the Wilson central terminal (preliminary results). *Physiol Meas* 34: 991–1012, 2013.
13. Dual SA, Ochsner G, Petrou A, *et al*: R-wave magnitude: A control input for ventricular assist devices. *Int Work Biosignal Interpret Osaka* c: 6–9, 2016.
14. Gargiulo GD: True unipolar ECG machine for Wilson central terminal measurements. *Biomed Res Int* 2015: 586397, 2015.
15. Dual S, Jacob D, Meboldt M, Daners M: Unipolar amplifier enabling measurement of far-field intra-cardiac eletromyogram for blood pump control. In Proc 14th Int Jt Conf Biomed Eng Syst Technol, *Biostec* 1: 40–48, 2021.
16. Dual SA, Schmid Daners M, Meboldt M, Jacob D, Pergantis P: Cardiac device, method and computer program product. 1–38, 2020. WO 2020/207840 A1.
17. Jenkins C, Bricknell K, Hanekom L, Marwick TH: Reproducibility and accuracy of echocardiographic measurements of left ventricular parameters using real-time three-dimensional echocardiography. *J Am Coll Cardiol* 44: 878–886, 2004.
18. Jenkins C, Moir S, Chan J, Rakhit D, Haluska B, Marwick TH: Left ventricular volume measurement with echocardiography: A comparison of left ventricular opacification, three-dimensional echocardiography, or both with magnetic resonance imaging. *Eur Heart J* 30:98–106, 2009.
19. Staufert S, Hierold C: Novel sensor integration approach for blood pressure sensing in ventricular assist devices. *In Procedia Eng* 168: 71–75, 2016.
20. Brancato L, Keulemans G, Verbelen T, Meyns B, Puers R. An implantable intravascular pressure sensor for a ventricular assist device. *Micromachines* 7:135, 2016.
21. Abraham WT, Adamson PB, Bourge RC, *et al*; CHAMPION Trial Study Group: Wireless pulmonary artery haemodynamic monitoring in chronic heart failure: A randomised controlled trial. *Lancet* 377: 658–666, 2011.
22. Dual SA, Zimmermann JM, Neuenschwander J, *et al*: Ultrasonic sensor concept to fit a ventricular assist device cannula evaluated using geometrically accurate heart phantoms. *Artif Organs* 43: 467–477, 2019.
23. Dual SA, Anthamatten L, Shah P, Meboldt M, Schmid Daners M: Ultrasound-based prediction of interventricular septum positioning during left ventricular support-an experimental study. *J Cardiovasc Transl Res* 13: 1055–1064, 2020.
24. Haines DE, Wong W, Canby R, *et al*: Validation of a defibrillation lead ventricular volume measurement compared to three-dimensional echocardiography. *Hear Rhythm* 14: 1515–1522, 2017.
25. Cysyk J, Newswanger R, Popjes E, *et al*: Cannula tip with integrated volume sensor for rotary blood pump control: Early-stage development. *ASAIO J* 65: 318–323, 2019.
26. Dual SA, Pergantis P, Schoenrath F, *et al*: Acute changes in preload and the QRS amplitude in advanced heart failure patients. *Biomed Phys Eng Express* 5: 045015, 2019.
27. Battler A, Froelicher VF, Gallagher KP, *et al*: Effects of changes in ventricular size on regional and surface QRS amplitudes in the conscious dog. *Circulation* 62: 174–180, 1980.
28. McFee R, Parungao A: An orthogonal lead system for clinical electrocardiography. *Am Heart J* 62: 93–100, 1961.